

Effect of Compaction Ratio, Frequency, Stress Amplitude and Cyclic Stress Ratio on the Dynamic Characteristic of Sea Sand Material under Vehicle Loading

C.L. Nguyen¹, H.H. Nguyen¹, Q.P. Nguyen¹, D.H. Ngo², and D.M. Nguyen¹

¹*Civil Engineering Department, University of Transport and Communications, Hanoi, Vietnam*

²*School of Civil Engineering, Suranaree University of Technology, 111 University Ave., Muang District, Nakhon Ratchasima 30000, Thailand*

E-mail: nguyenchaulan@utc.edu.vn

ABSTRACT: Haiphong city is situated on the North-Eastern coast of Vietnam. This city has a large coastal and sea area, which is an advantage for marine economic development. However, in order to reclaim the coastal area, river sand material is much demand which leads to face some environmental problems due to the exploitation of river sand. Thus, the intensive laboratory experiments were conducted including physical, chemical and mechanical tests of river sand and sea sand to evaluate the potential use of sea sand in road embankment in Haiphong city. The samples were prepared by compacting to value of 90% and 95% of maximum density defined by the Standard Proctor test. Consolidated undrained cyclic triaxial tests were conducted for sea sand samples and river sand samples. The cyclic triaxial test results showed that all samples are not liquefied under normal vehicle conditions which corresponding to cyclic deviator stress about 8 kPa and frequency of 1 Hz. In addition, sea sand samples were not liquefied when increasing the compaction effort to 95% of maximum density. Therefore, it is possible to use sea sand instead of river sand in some cases for reclamation land in the Haiphong area.

KEYWORDS: Dynamic properties, Road embankment, CU cyclic triaxial test, Liquefaction.

1. INTRODUCTION

Earthquakes and traffic loading are the most sources of cyclic loading, which may trigger the liquefaction of sandy ground leading to instability of foundations and existing structures (Hazout et al., 2017; Shivaprakash & Dinesh, 2017). Liquefaction phenomena is a natural disaster that happens due to loss of strength and stiffness of soils under cyclic loading conditions (Keramatikerman et al., 2017). The particles of granular soil having a tendency to move closer and the void space between particles will be reduced under vibration effect. As a consequence, the pore water pressure increases and the effective stress decreases, mostly in saturated soil (Lenart, 2008). On the other hand, the progressive build-up of pore water pressure may eventually become large enough, resulting in complete loss of shear strength accompanied by large deformation and failure. The liquefaction phenomena have been reported after earthquakes that occurred in 1964 at Niigata and Alaska, Japan, 1976 Tangshan, 2008 Wenchuan, China, and 2011 Tohoku Region Pacific Coast Earthquake, Japan (Bao et al., 2019).

On the other hand, several case studies in term of liquefaction induced by traffic loading have been reported (Carter, 1988; Griffin & Stanworth, 1985; Kaynia et al., 2000; Madshus et al., 1998). In most of these cases, the embankment failure was loose, saturated sand considered to be susceptible to liquefaction. Under traffic loading, the soil elements in subgrade are subjected to continuous principal stress rotation and the principal stresses of the soil element change in both magnitude and direction (Wu et al., 2017). During one certain loading circle, the vertical stress and shear stress in the soil shows different behavior (Ishikawa et al., 2011). The vertical stress reaches a peak and then decreases to zero value. While the shear stress changes not only in magnitude but also reverses in direction at the same time, leading to the rotation of principal stress axes, which plays an important role on the performance of pavement (Ishihara, 1983; Ishikawa et al., 2011; Tang et al., 2015).

Many studies have been conducted to investigate the effect of cyclic loading on sand behavior in laboratory testing. Cyclic triaxial tests have been the most common method used to characterize the cyclic behaviour of sands (Jefferies & Been, 2015). The liquefaction is defined in term of cyclic stress ratio to procedure a threshold strain of 5% double-amplitude (Ishihara, 1996) or 100% excess pore water pressure development in 20 cycles of uniform load application (Seed, 1979). The undrained cyclic triaxial test with no stress

reversal can also experience amount of strains, but the pore pressure ratio (the maximum excess pore water pressure / the vertical effective stress) does not necessarily reach 100 %. In addition, for silty sand, the pore water pressure ratio seems to be able to reach only 90 to 95%, which great strain amplitudes are observed (Ishihara, 1996). Sitharam, Ravishankar, and Vinod (2008) indicated that the potential for liquefaction of sand depends on the shear strain amplitude, initial compaction ratio, effective confining pressure and non-plastic fines. The compaction ratio increases, the liquefaction potential pressure decreases at a given confining pressure.

However, there has been an increase in the shortage of river sand material due to the rapid development of construction in recent years (Arulrajah et al., 2017). The high demand for river sand material lead to a major increase in sand mining in many areas and the extraction of sand from riverbank deposits has a detrimental effect on environmental problems. Consequently, it is necessary to use sea sand materials that can be considered to replace river sand materials in the construction industry especially road and bridge construction (Xiao et al., 2017). Even though, there are available studies reported that the sea sand material had been applied successfully as a raw construction material, the liquefaction behavior of sea sand materials under traffic loading condition is still limited recently (Dolage et al., 2013; Limeira et al., 2012; Xiao et al., 2017). In practice, the understanding of sea sand and river sand behavior under moving load has a profound effect on providing good design solutions and effective construction procedures for design engineers.

The objective of this study is to determine the liquefaction potential of sea sand and river sand sample at a compaction ratio corresponding to 90% and 95% of maximum dry density. In this paper, a series of undrained cyclic triaxial test was conducted for 18 samples including 15 sea sand and 3 river sand samples. The sea sand samples were collected in Hai Phong City area, in the North-Eastern coast of Vietnam. The river sand sample were collected in Hanam Province. These tests were considered the effect of compaction, frequency, stress amplitude and cyclic stress ratio on the dynamic characteristic of sea sand material under vehicle loading. The outcomes of this study will facilitate the design engineers to clearly understand the liquefaction behavior of sea sand and river sand sample under traffic loading condition.

2. EXPERIMENTAL INVESTIGATION

2.1 Testing Apparatus

To investigate the cyclic behavior of sand samples, the experiments were performed by using a cyclic triaxial shear test apparatus. The scheme of cyclic triaxial testing machine is shown in Figure 1. There are two options of loading system in this apparatus including; (a) ± 25 mm maximum with ± 5 kN double effect actuator; (b) ± 15 mm maximum with ± 14 kN double effect actuator. The advantages of this equipment are it can determine in both static conditions (effective stress and stress line) and cyclic condition. The used cyclic triaxial equipment remedies automatically the back pressure and cell pressure during cyclic loading test. The data is obtained by a computer-controlled data acquisition system. The axial deformation of the soil sample is measured by a linear variable differential transformer (LVDT) having the reading accuracy of 0.01 mm and 30 mm maximum deformation reading.

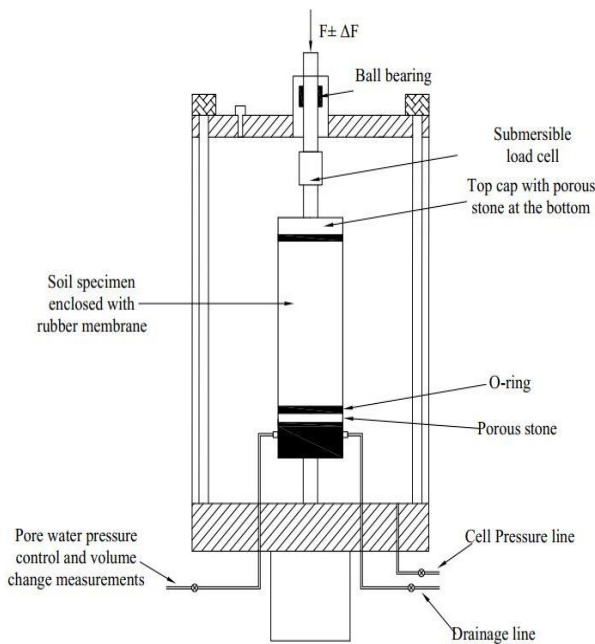


Figure 1 The scheme of cyclic triaxial testing machine

2.2 Material Samples

The sea sand samples were obtained from a construction project in Haiphong city, where is lack of river sand due to high demand for infrastructure. On the other hand, the river sand samples were collected in Hanam province. The grain size distribution curves for sea sand and river sand are shown in Figure 2.

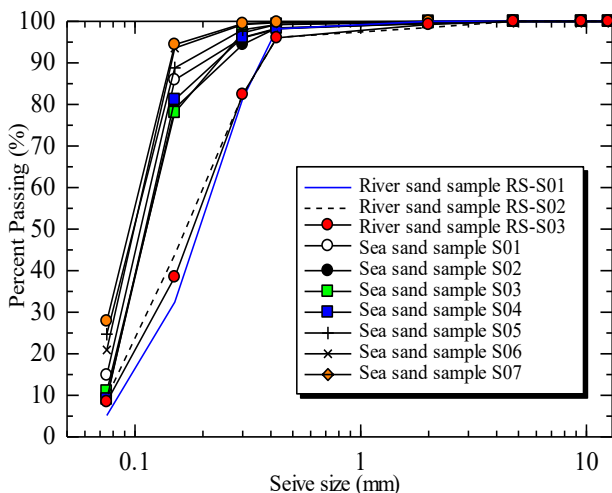


Figure 2 Particle size distribution of sea sand and river sand

The tested material contains 100% of sand. It is observed that the particle size of river sand samples is larger than those of sea sand samples. According to UCCS Standard, the sea sand and river sand are classified as medium sands (SW). The characteristics of tested materials are illustrated in Table 1. Both types of sand were prepared by compacting to the compaction ratio which is reached 90% and 95% of maximum dry density. The compaction ratio is defined as the ratio between dry density in the field and maximum dry density which were conducted by using laboratory Standard Proctor test (ASTM D698).

The maximum dry density varied from 1.584 to 1.644 g/cm³ and 1.651 to 1.713 g/cm³ for sea sand and river sand, respectively. In addition, California Bearing Ratio of sand was also conducted according to Standard Method of Test for The California Bearing Ratio (AASHTO T193). The results showed that the minimum California Bearing Ratio value of sea sand and river sand sample at a compaction ratio of 95% are 10.8 and 13.2, respectively, which meets the requirements of CBR value for subgrade layer in AASHTO standard (AASHTO, 2004).

Table 1 Initial characteristic of sand samples

No.	Group of Samples	Samples	Compaction Ratio	Max Dry Density g/cm ³	γ_s g/cm ³	Note
1	Group 1	S01	0.95	1.644	2.58	Sea sands
2		S02	0.90	1.644	2.58	
3		S03	0.95	1.644	2.58	
4	Group 2	S04	0.90	1.631	2.58	
5		S05	0.90	1.631	2.58	
6		S06	0.90	1.631	2.58	
7	Group 3	S07	0.90	1.584	2.57	
8		S08	0.90	1.584	2.57	
9		S09	0.90	1.584	2.57	
10	Group 4	S10	0.95	1.584	2.57	
11		S11	0.95	1.584	2.57	
12		S12	0.95	1.584	2.57	
14	Group 5	S13	0.90	1.597	2.675	
15		S14	0.95	1.682	2.675	
17		S15	0.95	1.676	2.674	
21	Group 6	R01	0.95	1.651	2.590	River sands
22		R02	0.90	1.713	2.570	
23		R03	0.90	1.681	2.590	

2.3 X-ray Diffraction Analysis

The X-ray diffraction (XRD) analysis was conducted for river sand and sea sand sample before testing. The XRD test results of river sand and sea sand samples were plotted in Figure 3. The X-ray

diffraction analysis results of sea sand and river sand sample showed that the sand sample (both sea sand and river sand) is composed mainly of Quartz mineral (Silicon dioxide SiO₂). The Quartz mineral content of sea sand samples was 50%, which was higher than those of river sand (41-47%). A small amount of clay mineral (Illite, Kaolinite, chlorite) was also presented. The result of X-ray diffraction analysis also indicated that the clay mineral in sea sand sample was lower than those of river sand.

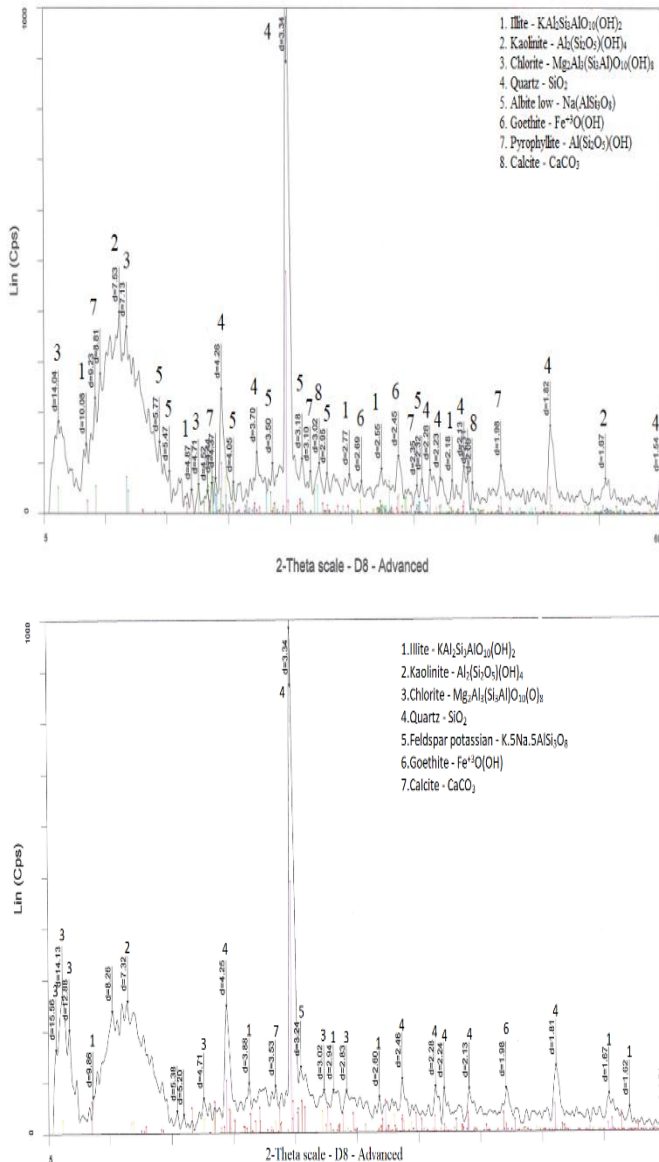


Figure 3 X-ray diffraction analysis results a) sea sand material, b) river sand materials.

2.4 Sample Preparation for Undrained Cyclic Triaxial Test

The stress-controlled cyclic triaxial tests were conducted under undrained conditions, which could be accepted as some cases with dynamic loadings such as earthquake condition or vehicle loading. The remolded specimens including 15 sea sand and 3 river sand samples were conducted the cyclic triaxial test in this study. The triaxial specimens of 70 mm diameter and 140 mm in height were prepared by using the wet-pouring method, which was proposed by R. Ladd (1978). The procedure of wet-pouring method incorporates a tamping method of compacting moist coarse-grained sand in layers. Each layer was compacted with optimal moisture content to ensure that the sample was reached the compaction ratio corresponding with 90% and 95% of maximum dry density.

After the replacement of the specimens in the triaxial cell, three basic stages of the cyclic triaxial test were performed: saturation process, consolidation process and cyclic loading process. In the saturation step, back pressure (σ_{back}) of 90 kPa and cell pressure (σ_{cell}) of 100 kPa were carried out until it reached the Skempton value that is normally greater than 0.95. The Skempton or B value as parameter shows that only the fully saturated sample is used in the experiment. For the next stage, the sample was consolidated with cell pressure (σ_{cell}) of 70 kPa, back pressure (σ_{back}) of 130 kPa and 40 kPa the effective stress (σ'_3). The detail testing conditions for each sample is shown in Table 2. The cyclic stress ratio (CSR) is defined as the ratio of desired deviator stress to double the effective consolidation stress (ASTM D 5311-92). After finish consolidation steps, the valve was closed to ensure that no water dissipated during the loading process. In the final step, the sample was subjected to dynamic loading by acting axial cyclic stress ($\pm\sigma_{d1}$) with a different amplitude of shear strain and changing frequency. The value of $\pm\sigma_{d1}$ on the cyclic triaxial test represents $\pm\tau$ on a horizontal area of soil mass element which represents soil shear stress due to cyclic loading which acts on it. During the test, pore water pressures, cell pressure, axial strain and axial stress were recorded continuously. To study the failure mechanism of sea sand sample under traffic loading condition, the number of dynamic loading tests were conducted with difference amplitude (8-32 kPa) which corresponding to the maximum value that can be reached for road embankment location at 1.5 m depth compared with pavement surface.

In this paper, two main conditions were taken into account during the cyclic triaxial test as follows:

- Consider the effect of stress amplitude on liquefaction (determine the failure mechanism of the sand sample during the cyclic loading). In this condition, 6 sea sand samples (S01-S06) were conducted the cyclic loading test with the changing of stress amplitude (8 ± 32 kPa) and a constant value of frequency ($f = 1$ Hz).
- Consider the effect of frequency on liquefaction (determine the stability of material when the vehicles are moving on the road) in case of different speed with changing of frequency ($f = 1-8$ Hz), but stress amplitude remained constant (± 8 kPa) for sample S07 – S12.

Base on the test result of cyclic triaxial test, the liquefaction phenomena can be determined by considering the increase of pore water pressure reaches 95% of initial stress (Figure 4a) or the development of large deformation, are described with amplitude corresponding with 5% of axial strain (Figure 4b) (Ishihara, 1993). For establishing the liquefaction of specific sample (up to 95% of pore water pressure or 5% amplitude axial strain), the number of cycles must be indicated in a particular case with the uniform dynamic loading amplitude. It is noted that to reach the liquefaction stage corresponding to the 95% of pore water pressure and 5% of axial shear strain, both of this condition could not occur at the same time, and then two separate curves can be drawn (Figure 4c).

Table 2 The cyclic triaxial test for samples

Sample	Frequency (f)	Cell pressure σ_3 (kPa)	Back pressure σ_b (kPa)	Effective stress σ'_c (kPa)	Stress amplitude σ_a (kPa)	Cyclic stress Ratio (CSR)
S01	1	60	20	40	32	0.4
S02	1	60	20	40	24	0.3
S03	1	170	130	40	16	0.2
S04	1	170	130	40	8	0.1
S05	1	170	130	40	16	0.2
S06	1	170	130	40	24	0.3
S07	1	170	130	40	8	0.1
S08	2	170	130	40	8	0.1
S09	3	170	130	40	8	0.1
S10	1	170	130	40	8	0.1

S11	2	170	130	40	8	0.1
S12	3	170	130	40	8	0.1
S13	1	150	108	42	16	0.1
S14	1	170	130	40	16	0.2
S15	8	150	108	42	16	0.1
R01	1	170	130	40	8	0.1
R02	1	170	130	40	8	0.1
R03	1	170	107	63	16	0.13

10, and also summarized in Table 3. The relationship between the pore pressure ratio (R_u %) and the number of loading cycles for sea sand sample subjected to single stress amplitude of 8 kPa, 16 kPa, 24 kPa, and 32 kPa (Figure 5 to Figure 10). It is evident that the pore water pressure ratio increased with the increase of stress amplitude (Figure 5, Figure 6, Figure 7). For group 1 with the sea sand sample of 90% and 95 % of compaction ratio, it is evident that the liquefaction phenomena did not occur on the sea sand sample of 95 % of compaction ratio even the sample S01 was subjected the large vibration amplitude of 32 kPa (Figure 5, Figure 6, Figure 7). The maximum pore water pressure ratio for sample S01 and S03 are approximately 77.5%, 21.0 % at the stress amplitude 32 kPa and 16 kPa, respectively. The liquefaction phenomena were found on the Sample S02 (90% of compaction ratio) under 24 kPa of stress amplitude. The pore water pressure ratio developed gradually during the first 40 cycles and reached 95% in the 95th cycles.

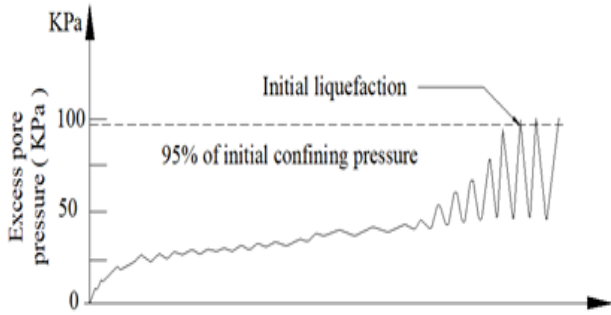


Figure 4a

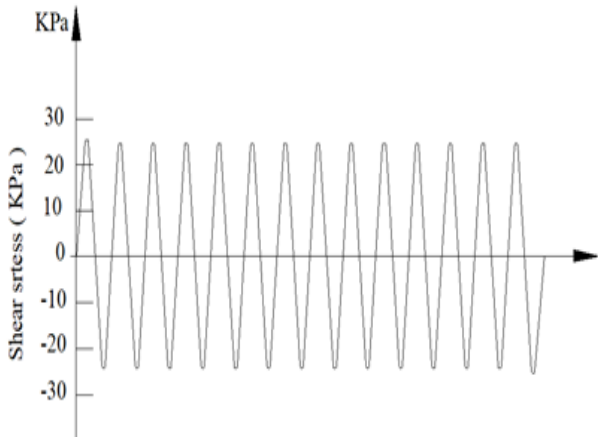


Figure 4b

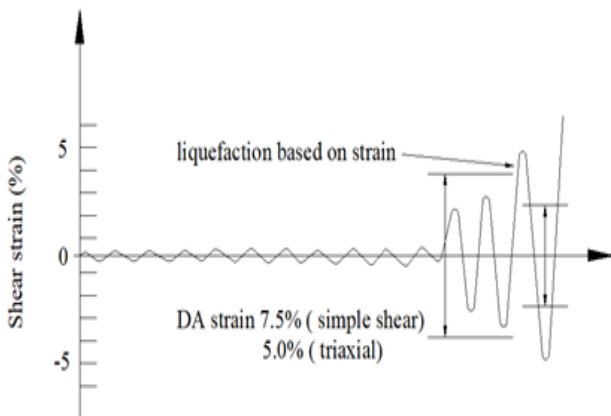


Figure 4 Liquefaction evaluation method.

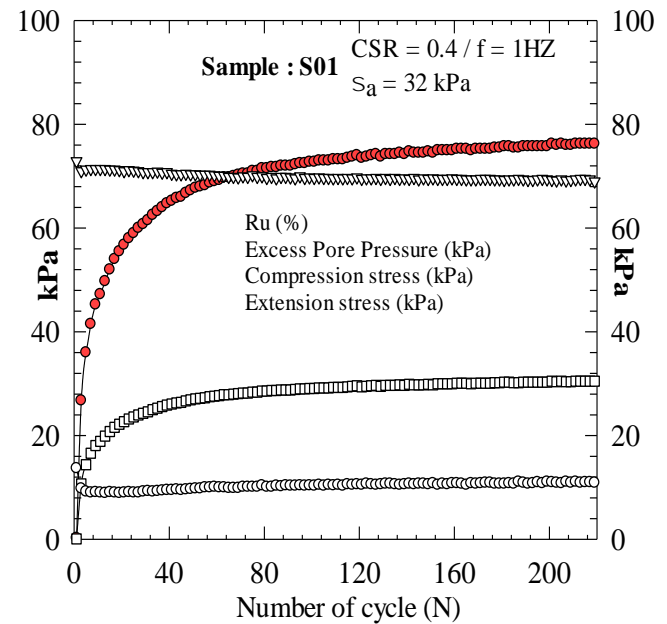


Figure 5 Cyclic triaxial test results of Sample S01

On the other hand, the liquefaction phenomena were found on the sample S05 and S06 at stress amplitude 16 and 24 kPa with compaction ratio of 0.90 in group 2 (Figure 8 to Figure 10). The similar result has been found in sample S02. It means that when stress amplitude varied from 8 to 32 kPa, the sea sand sample (compaction ratio is 0.9) was not liquefied at the lowest stress amplitude (8 kPa) but liquefied at vibration amplitude of 16 kPa and 24 kPa (Figure 9 and 10). The maximum pore water pressure ratio for all the liquefied sand samples are higher than 95% at the stress amplitude 16 and 24 kPa. The behavior of samples, which were 90% and 95% of compaction ratio indicated that the compaction ratio has been considered as a dominant factor influencing the cyclic strength as studied by (R. S. Ladd, 1974; Mulilis et al., 1977; Tatsuoka et al., 1986).

The effect of confining pressure on liquefaction potential can be considered in sea sand sample S02 and S06 at the same cyclic stress ratio, frequency, and stress amplitude with confining pressure ranging from 60 kPa to 170 kPa. Based on the build-up of pore pressure ratio, it proves that the confining pressure has a significant effect on the liquefaction potential. At low confining pressure (60 kPa), the liquefaction failure occurred on the sample S02 after 95 cycles. On the other hand, the pore pressure ratio tested on sample S06 increases rapidly during the first 3 cycles when its subjected 170 kPa of confining pressure. The potential for liquefaction is found to decrease with increase in the confining pressure. The results of the present study are similar to the results reported by Sitharam et al. (2008) and Dobry, Ladd, Yokel, Chung, and Powell (1982).

3. RESULTS AND DISCUSSIONS

3.1 Effects of Stress Amplitude on the Liquefaction

To determine the failure mechanism of the sand sample during the cyclic loading, two main groups have been divided such as group 1 and group 2 (Table 3). Each group including 3 sea sand samples were conducted cyclic triaxial tests under the condition that the frequency value was remained constant ($f=1$ Hz) and the stress amplitude changed from 8 to 32 kPa. In this condition, the test results of the cyclic loading test are presented in Figure 5 to Figure

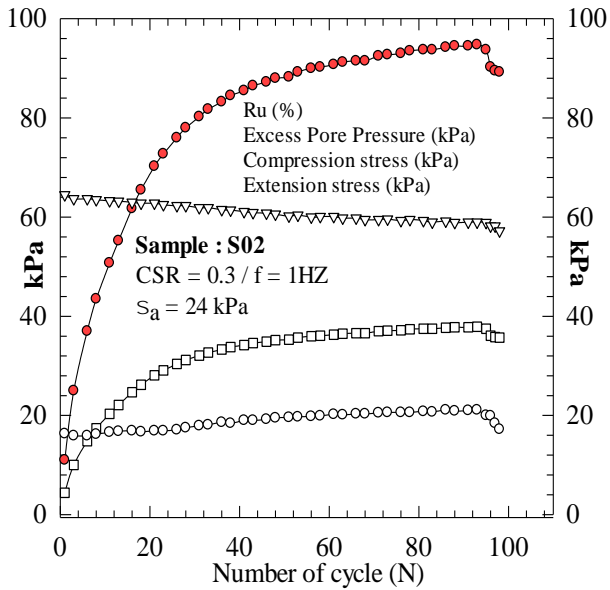


Figure 6 Cyclic triaxial test results of Sample S02

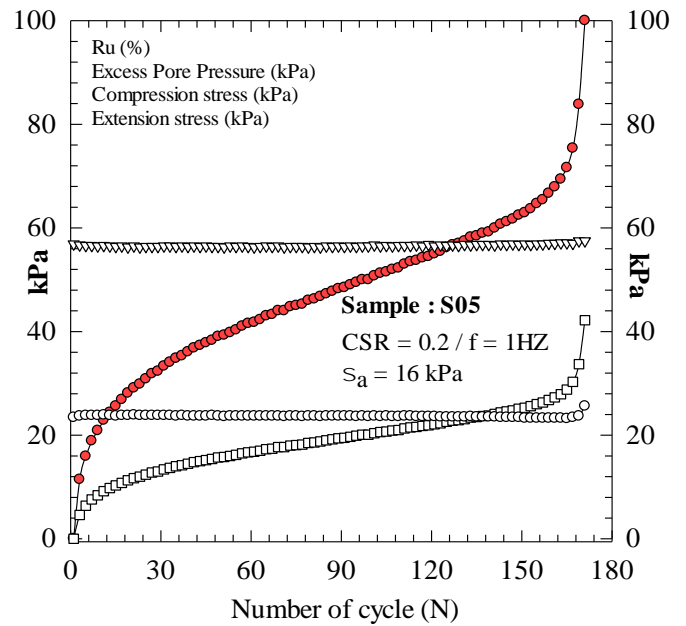


Figure 9 Cyclic triaxial test results of Sample S05

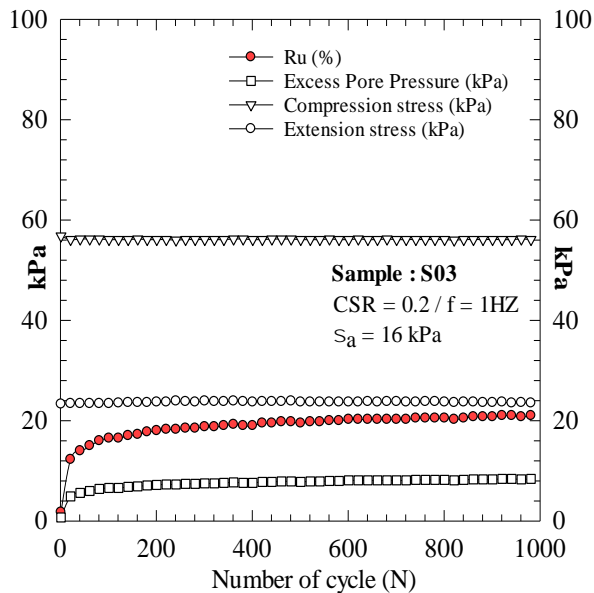


Figure 7 Cyclic triaxial test results of Sample S03

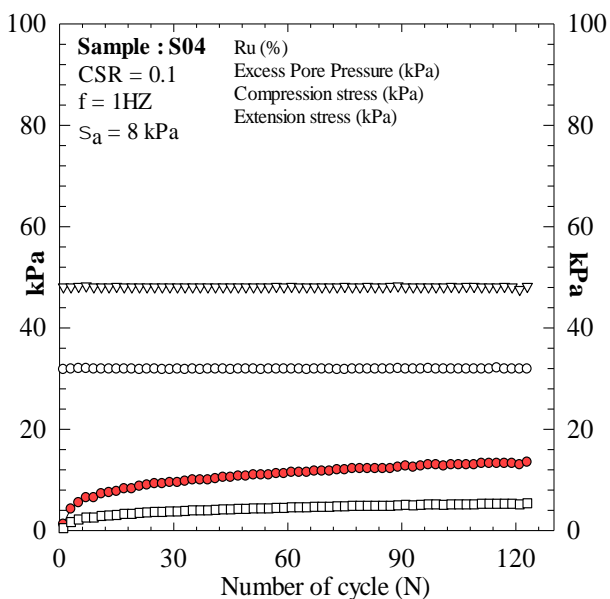


Figure 8 Cyclic triaxial test results of Sample S04

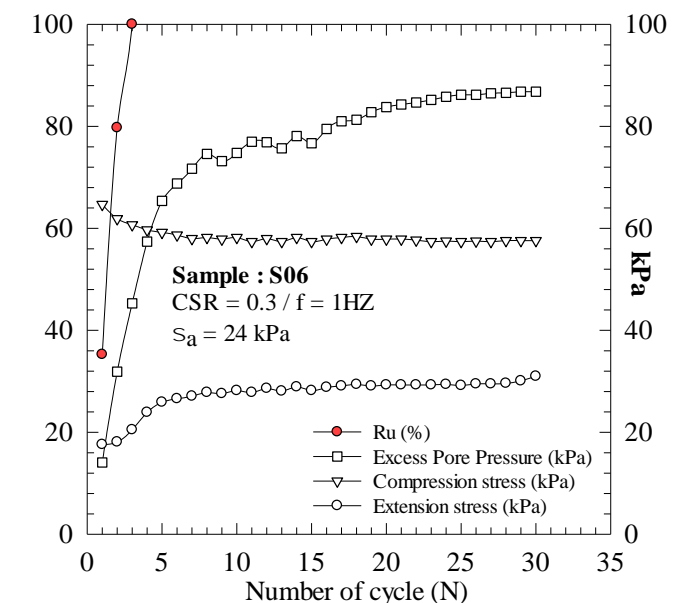


Figure 10 Cyclic triaxial test results of Sample S06

Table 3 Summary of test results to determine failure mechanism

Group of sample	Sample	Compaction Ratio	Freq. f (Hz)	Stress amp. σ_a (kPa)	Ru (%)	Comment
Group 1	S01	0.95	1	32	77.5	Not liquefied
	S02	0.90	1	24	95.0	Liquefied
	S03	0.95	1	16	21.0	Not liquefied
Group 2	S04	0.90	1	8	13.5	Not liquefied
	S05	0.90	1	16	100	Liquefied
	S06	0.90	1	24	100	Liquefied

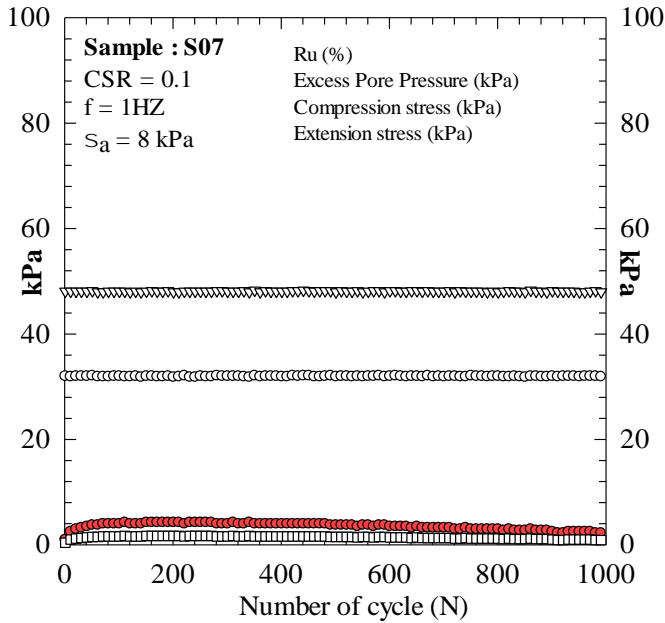


Figure 11 Cyclic triaxial test results of Sample S07

3.2 Effects of Frequency on the Liquefaction

In this case, to study vehicles capacity moving on the road with difference velocity, the vibration amplitude was kept constant while the frequency f (Hz) varies to check the liquefaction potential corresponding to the samples having 90% and 95% of compaction ratio. There are 3 main groups of sample in this case (Table 4). Group 4 consists of 3 sea sand samples (S07 –S09) with 90% of compaction ratio. Group 5 (S10-S12) includes 3 sea sand samples, which are 95% of the compaction ratio. Group 4 and 5 were tested at the stress amplitude of 8 kPa and the frequency varied from 1 to 3 Hz. Group 6 (S13-S15) is the combination of samples with 90% and 95% of the compaction ratio. In group 6, the sea sand samples were carried out to test the triaxial cyclic loading test at 16 kPa of stress amplitude with the changing of frequency from 1 to 8 Hz. In addition, sand samples (S07 – S15) have been tested in this case to study the effect of frequency on the liquefaction capacity. The test results of the cyclic triaxial test are plotted in Figure 11 to Figure 19. The summary form is also shown in Table 4.

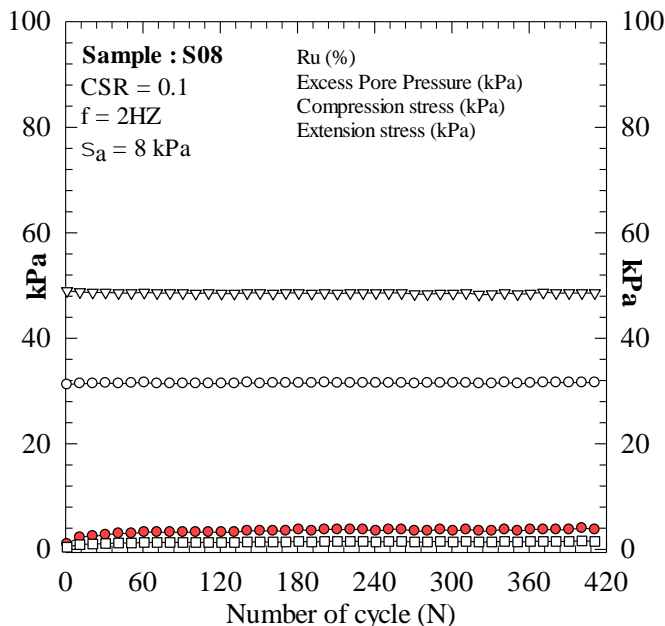


Figure 12 Cyclic triaxial test results of Sample S08

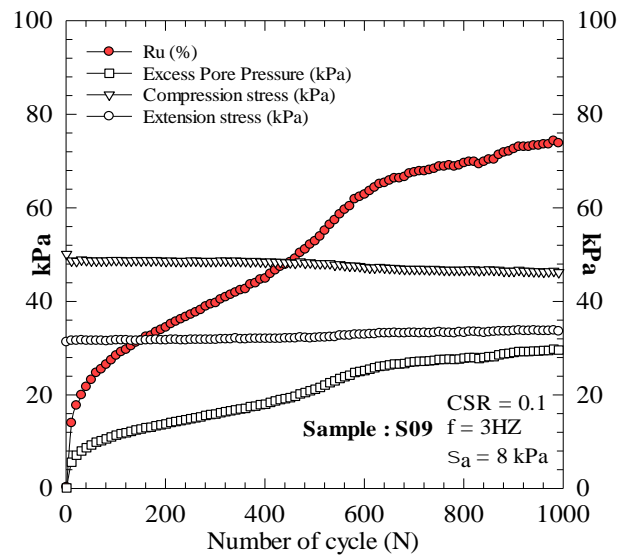


Figure 13 Cyclic triaxial test results of Sample S09

Figure 11 to Figure 13 shows the pore pressure ratio and the number of cycles of the sea sand sample in group 4 with 90% of compaction ratio under different frequency. When the sea sand samples were tested under 8 kPa of stress amplitude and frequency less than 2 Hz, the pore pressure ratio shows a rapid increase that eventually slows and then plateaus. The pore pressure generation increases sharply and reaches 77% of pore pressure ratio at approximately the 1000th cycle in case of when the frequency is 3. However, when the frequency varies from 1 to 3 under the 8 kPa of stress amplitude, the liquefaction failure did not occur in this group. The similar behavior has been found in the sample S10, S11, S12, S14, and S15. The test results proves that the changing of frequency does not have much effect on the liquefaction of sea sand samples with 95% of compaction ratio.

The effect of stress amplitude on the sea sand sample with 90% of compaction ratio is discussed in the previous section. The liquefaction failure can be seen in the sample S13 as plotted in Figure 17. The pore pressure ratio increases rapidly and the failure occurs at approximately the 120th cycles. This finding is similar to the results of sea sand sample R0.9 tested at the same condition ($f=1$ Hz, $\sigma_a = 16$ kPa) in the previous section.

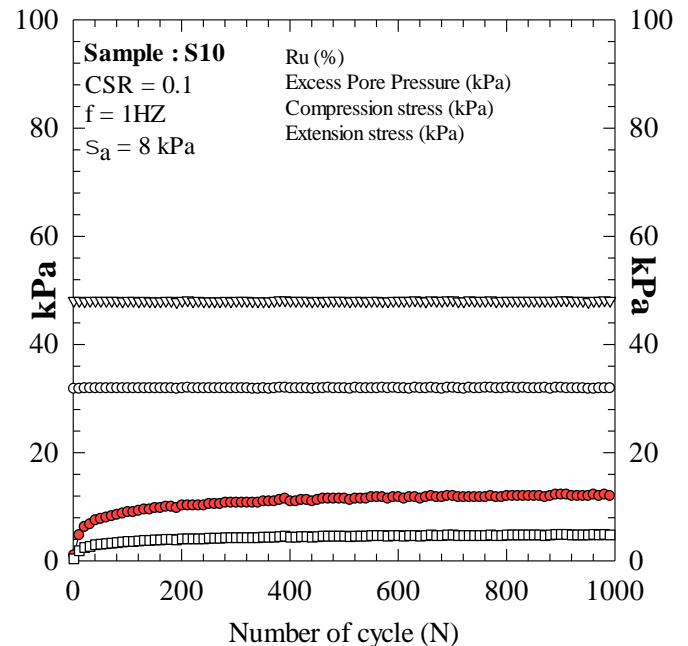


Figure 14 Cyclic triaxial test results of Sample S10

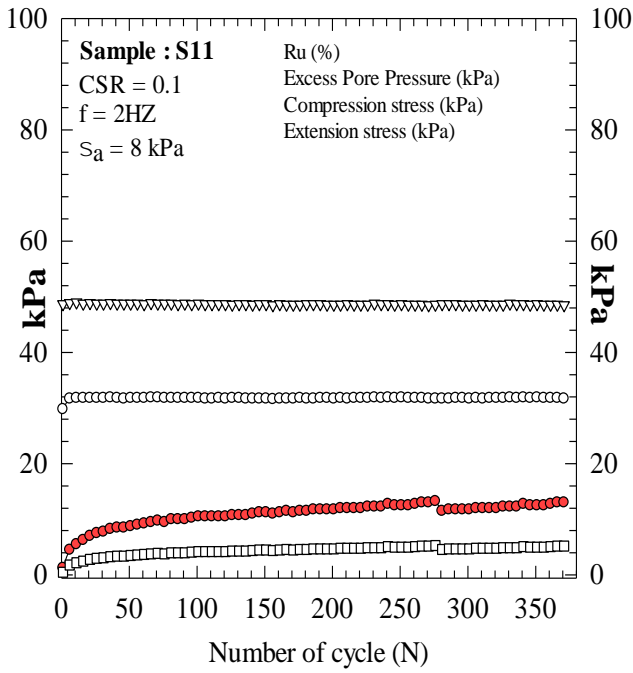


Figure 15 Cyclic triaxial test results of Sample S11

Table 4 Summary of test results in different speed of vehicles testing conditions

Group of sample	Sample	Compaction Ratio	Freq. f (Hz)	Stress amp. σ_a (kPa)	Ru (%)	Comment
Group 4	S07	0.90	1	8	4.5	Not liquefied
	S08	0.90	2	8	4.0	Not liquefied
	S09	0.90	3	8	74.3	Not liquefied
Group 5	S10	0.95	1	8	13.0	Not liquefied
	S11	0.95	2	8	13.3	Not liquefied
	S12	0.95	3	8	17.0	Not liquefied
Group 6	S13	0.90	1	16	100.0	Liquefied
	S14	0.95	1	16	40.0	Not liquefied
	S15	0.95	8	16	41.5	Not liquefied

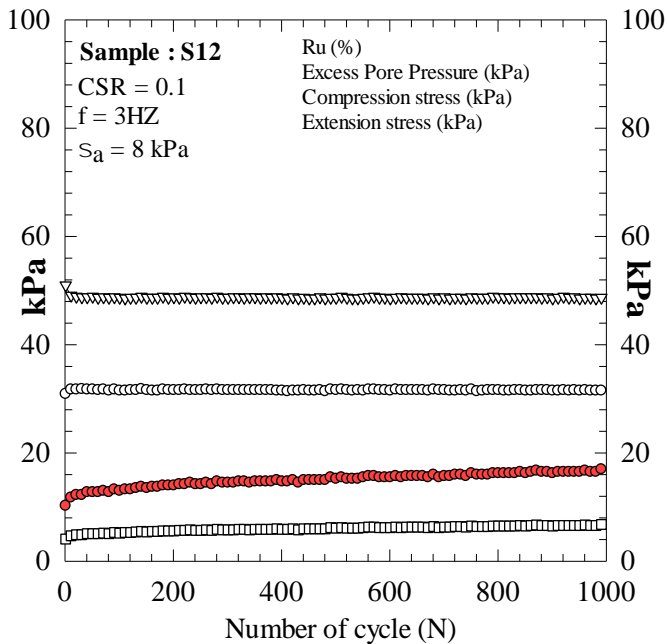


Figure 16 Cyclic triaxial test results of Sample S12

3.3 Comparison of Sea and River Sand Samples

Sea sand and river sand samples are compared based on the cyclic triaxial test results which corresponding to frequency of 1 Hz and a density ratio of R90, and R95. The results of tested river sand are shown in Figure 20 to Figure 22 and summarized in Table 5. Based on the test result summarized in Table 5 and Table 6, it proofs that all sea sand and river sand samples were not liquefied under normal condition of vehicles moving on the road (stress amplitude (σ_a) of 8 kPa and frequency of 1 Hz). River sand samples could be subjected under the condition that the vibration amplitude is twice higher than those in the normal condition of vehicles moving on the road.

On the other hand, sea sand samples R90 are liquefied when the vibration amplitude is twice higher than those in the normal condition of vehicles moving on the road and it was liquefied under cyclic stress ratio (CSR) varying from 0.1 to 0.3. Thus, in the case of embankment having compaction ratio larger than 95% corresponding to normal amplitude or the value of amplitude is twice higher than normal conditions, the embankment will not occur liquefaction state.

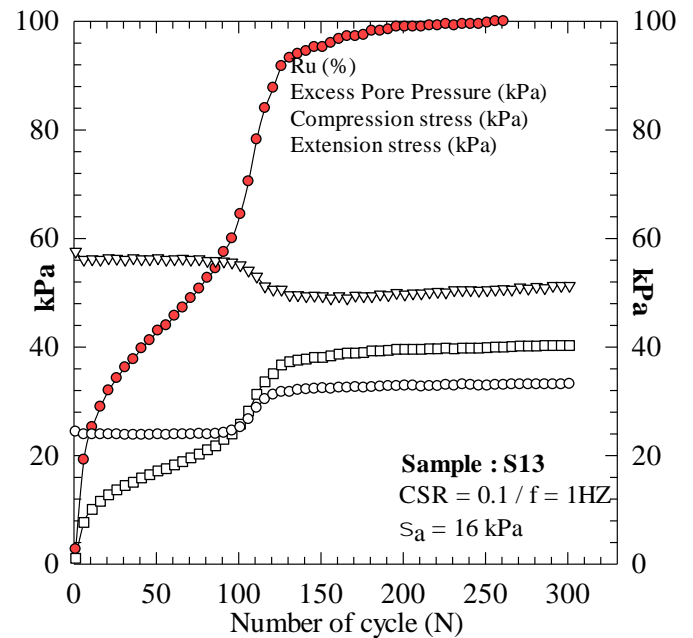


Figure 17 Cyclic triaxial test results of Sample S13

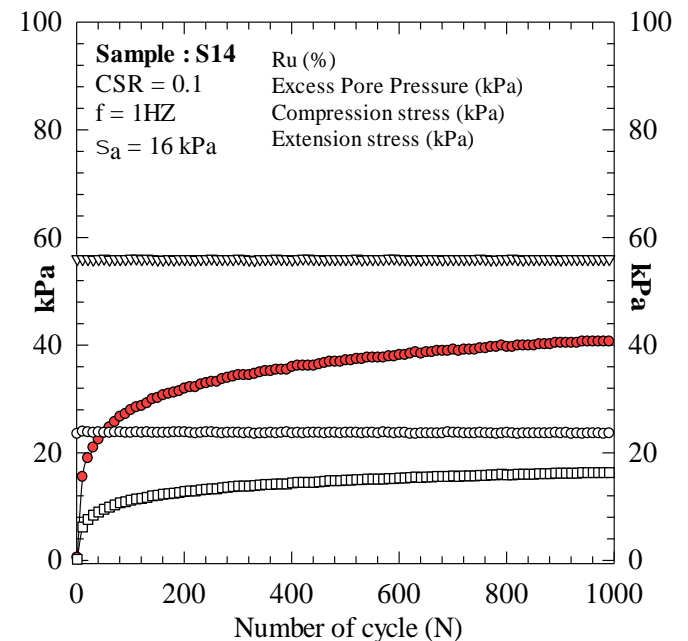


Figure 18 Cyclic triaxial test results of Sample S14

Table 5 Summary of test result for river sand

Sample	Compaction ratio	Frequency f(Hz)	Stress amp. σ_a (kPa)	Cyclic stress Ratio (CSR)	R_u	Comment
R01	0.95	1	8	0.1	32	Not Liquefied
R02	0.90	1	8	0.1	8.25	Not Liquefied
R03	0.90	1	16	0.2	60	Not Liquefied

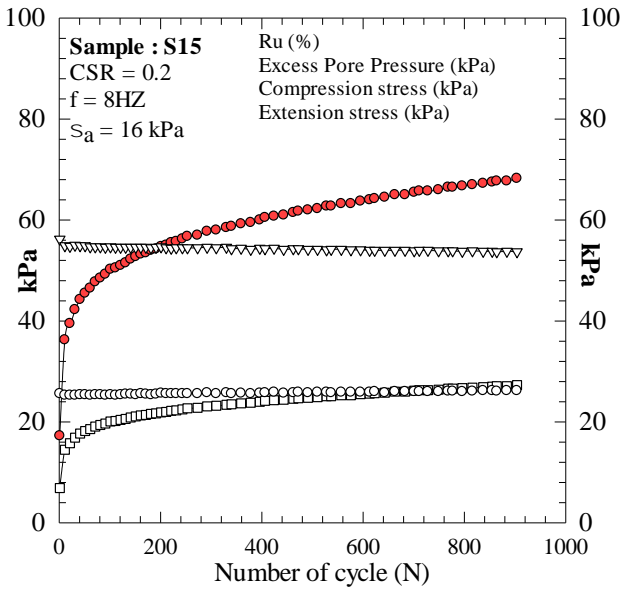


Figure 19 Cyclic triaxial test results of Sample S15

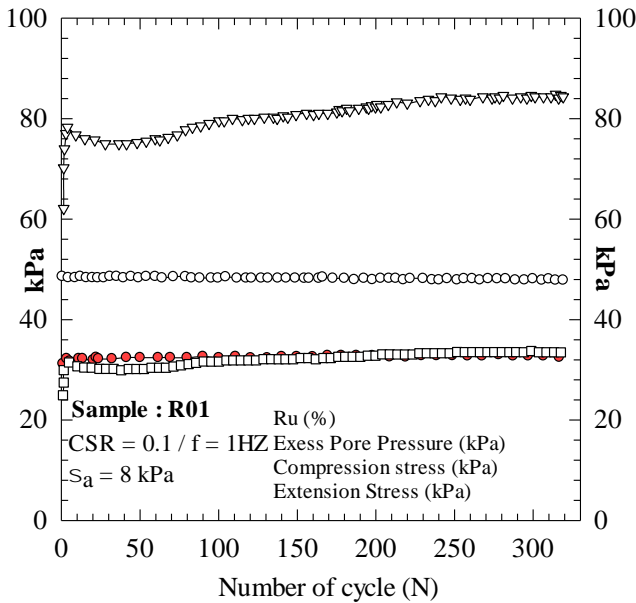


Figure 20 Cyclic triaxial test results of Sample R01

Table 6 Comparison of test results between sea sand and river sand samples

Sample	Compaction Ratio	Freq. f (Hz)	Stress amp. σ_a (kPa)	Cyclic stress Ratio (CSR)	R_u	Comment
R01	0.95	1	8	0.1	32.0	Not liquefied
R02	0.90	1	8	0.1	8.25	Not liquefied

Sample	Compaction ratio	Frequency f(Hz)	Stress amp. σ_a (kPa)	Cyclic stress Ratio (CSR)	R_u	Comment
R03	0.90	1	16	0.2	60.0	Not liquefied
S03	0.95	1	16	0.2	8.0	Not liquefied
S04	0.90	1	8	0.1	13.5	Not liquefied
S05	0.90	1	16	0.2	100.0	Liquefied
S07	0.90	1	8	0.1	4.5	Not liquefied
S10	0.95	1	8	0.1	13.0	Not liquefied
S13	0.90	1	16	0.1	100.0	Liquefied
S14	0.95	1	16	0.2	100.0	Liquefied

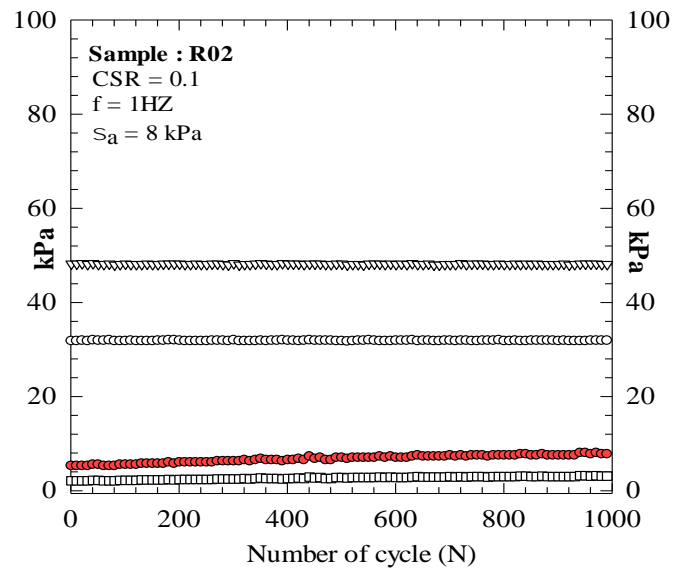


Figure 21 Cyclic triaxial test results of Sample R02

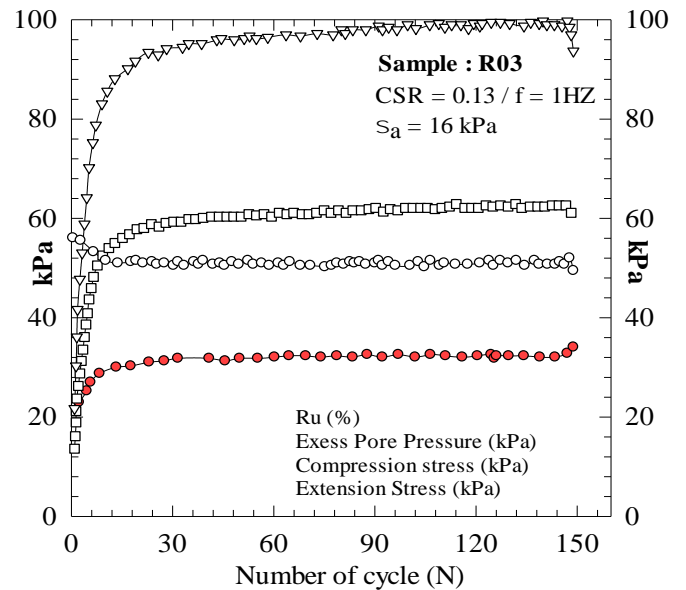


Figure 22 Cyclic triaxial test results of Sample R03

4. CONCLUSIONS

This article presents a study on the effect of compaction on liquefaction of river and sea sand in Hai Phong City, Viet Nam. Based on the test result of cyclic loading conducted under 2 main

conditions are discussed above. The conclusions can be drawn as follows:

- 1) The potential liquefaction of sea sand sample depends on the compaction ratio, stress amplitude, frequency, and the initial effective confining pressure. The increase of confining pressure decreases the liquefaction potential of the sea sand sample having 90% of compaction ratio under the same frequency, cyclic stress ratio and stress amplitude.
- 2) All of sea sand and river sand sample are not liquefied under normal vehicle moving condition with the compaction ratio, which is higher than 90%.
- 3) Sea sand samples having the compaction ratio R90 are liquefied under the vibration amplitude, which is twice higher than the normal condition of vehicle moving (8 kPa). In the case of embankment having compaction ratio larger than 95%, the embankment will not be occurred the liquefaction failure at any stress amplitude (8-32 kPa)
- 4) It is recommended that that in the case of embankment having compaction ratio R90 and R95, the embankment will not be liquefied under normal amplitude value. Thus the sea sand can be used to replace river sand for road embankment material.

5. REFERENCES

- AASHTO T. Standard method of test for moisture-density relations of soils using a 2.5-kg (5.5-lb) rammer and a 305-mm (12-in.) drop. Standard Specifications for Transportation Materials and Methods of Sampling and Testing 2004: 99-01.
- ASTM D 5311-92. Standard test method for load controlled cyclic triaxial strength of soil. Annual Book of ASTM Standards, American Society for Testing and Materials 2004: 1-10.
- Arulrajah, A., Yaghoobi, E., Wong, Y. C., and Horpibulsuk, S. (2017) "Recycled plastic granules and demolition wastes as construction materials: Resilient moduli and strength characteristics", *Construction and Building Materials*, 147, pp639-647.
- Bao, X., Jin, Z., Cui, H., Chen, X., and Xie, X. (2019) "Soil liquefaction mitigation in geotechnical engineering: An overview of recently developed methods", *Soil Dynamics and Earthquake Engineering*, 120, pp273-291.
- Carter, D. P. (1988) "Liquefaction potential of sand deposits under low levels of excitation", California Univ., Berkeley, CA (USA).
- Dobry, R., Ladd, R., Yokel, F., Chung, R. M., and Powell, D. (1982) "Prediction of pore water pressure buildup and liquefaction of sands during earthquakes by the cyclic strain method", National Bureau of Standards Gaithersburg, MD.
- Dolage, D. A., Dias, M. G. J., Ariyawansa, C. T. (2013) "Offshore sand as a fine aggregate for concrete production", *British Journal of Applied Science & Technology*, 3(4), p813.
- Griffin, M. J., and Stanworth, C. G. (1985) "Generation and perception of vibration from rail traffic", In *Track Technology: Conference of the Institute of Civil Engineers*.
- Hazout, L., Zitouni, Z. E. B., Belkhatir, M., and Schanz, T. (2017) "Evaluation of Static Liquefaction Characteristics of Saturated Loose Sand Through the Mean Grain Size and Extreme Grain Sizes", *Geotechnical and Geological Engineering*, 35(5), pp2079-2105.
- Ishihara, K. (1983) "Soil response in cyclic loading induced by earthquakes", traffic and waves. Proc. 7th Asian Reg. Conf. Soil Mech. Found. Eng.
- Ishihara, K. (1983) "Liquefaction and flow failure during earthquakes", *Geotechnique*, 43(3), pp351-451.
- Ishihara, K. (1996) "Soil behaviour in earthquake geotechnics", Offord Clarendon Press.
- Ishikawa, K., Tatsuoka, F., and Yasuda, S. (2011) "Cyclic deformation of granular material subjected to moving-wheel loads", *Canadian Geotechnical Journal*, 48(5), pp691-703.
- Jefferies, M., and Been, K. (2015) "Soil liquefaction: a critical state approach", CRC press.
- Kaynia, M., Madshus, C., and Zackrisson, P. (2000) "Ground vibration from high-speed trains: prediction and countermeasure", *Journal of geotechnical and geoenvironmental engineering*, 126(6), pp531-537.
- Keramatikerman, M., Chegenizadeh, A., and Nikraz, H. (2017) "Experimental study on effect of fly ash on liquefaction resistance of sand", *Soil Dynamics and Earthquake Engineering*, 93: pp1-6.
- Ladd, R. (1978) "Preparing test specimens using undercompaction", *Geotechnical Testing Journal*, 1(1), pp16-23.
- Ladd, R. (1974) "Specimen preparation and liquefaction of sands", *Journal of geotechnical and geoenvironmental engineering*, 100.
- Lenart, S. (2008) "The response of saturated soils to a dynamic load", *Acta Geotechnica Slovenica*, 5(1), pp37-49.
- Limeira, J., Agullo, L., and Etxeberria, M. (2012) "Dredged marine sand as a new source for construction materials", *Materiales de Construcción*, 62(305), pp7-24.
- Madshus, C., Kanynia, A. M., Harvik, L., and Holme, J. K. (1998) "A numerical ground model for railway-induced vibration", *Ground dynamics and manmade processes: prediction, design and management*. Thomas Telford: Institution of Civil Engineers, Ground Engineering Board, pp45-55.
- Mulilis, J. P., Arulanandan, K., Mitchell, J. K., Chan, C. K., and Seed, H. B. (1997) "Effects of sample preparation on sand liquefaction", *Journal of the Geotechnical Engineering Division*, 103(2), pp91-108.
- Seed, B. (1979) "Soil liquefaction and cyclic mobility evaluation for level ground during earthquakes", *Journal of geotechnical and geoenvironmental engineering*, 105(ASCE 14380).
- Shivaprakash, B. G., and Dinesh, S. V. (2017) "Dynamic Properties of Sand-Fines Mixtures", *Geotechnical and Geological Engineering*, 35(5), pp2327-2337.
- Sitharam, T. G., Ravishankar, B. V., and Vinod, J. (2008) "Liquefaction and pore water pressure generation in sand - A cyclic strain approach", *Journal of Earthquake and Tsunami*, 2(03), pp227-240.
- Tang, L., Chen, H., Sang, H., Zhang, S., and Zhang, J. (2015) "Determination of traffic-load-influenced depths in clayey subsoil based on the shakedown concept", *Soil Dynamics and Earthquake Engineering*, 77, pp182-191.
- Tatsuoka, F., Ochi, K., Fujii, S., and Okamoto, M. (1986) "Cyclic undrained triaxial and torsional shear strength of sands for different sample preparation methods", *Soils and Foundations*, 26(3), pp23-41.
- Wu, T., Cai, Y., Guo, L., Ling, D., and Wang, J. (2017) "Influence of shear stress level on cyclic deformation behaviour of intact Wenzhou soft clay under traffic loading", *Engineering Geology*, 228, pp61-70.
- Xiao, J., Qiang, C., Nanni, A., and Zhang, K. (2017) "Use of sea-sand and seawater in concrete construction: Current status and future opportunities", *Construction and Building Materials*, 155: 1101-1111.